crystals

MDPI

Article

Effects of Pressure and Cooling Rates on Crystallization Behavior and Morphology of Isotactic Polypropylene

Vito Speranza *, Rita Salomone and Roberto Pantani

Department of Industrial Engineering, University of Salerno, via Giovanni Paolo II, 132, 84084 Fisciano, SA, Italy; rsalomone@unisa.it (R.S.); rpantani@unisa.it (R.P.)
* Correspondence: vsperanza@unisa.it

Abstract: Isotactic Polypropylene (iPP) is a widely used polymer due to its excellent mechanical and thermal properties, as well as its chemical resistance. The crystallization behavior of polypropylene is influenced by several factors, such as temperature, cooling rate, and pressure. The effect of pressure is significant for both scientific and technological points of view, since in important industrial processing techniques the polymer solidifies under high pressures. In this paper, the study of the effect of pressure on the crystallization kinetics of iPP was conducted using a dilatometer in the pressure range from 100 to 600 bar and under two cooling rates: 0.1 and 1 °C/s. The morphology of the samples was characterized using DSC, optical microscopy, and X-ray diffraction. The results showed that pressure had a larger effect on specific volume changes at higher temperatures (in the melt state) than at lower temperatures (in the solid state). The polymer crystallization, which determined the transition between the melt and solid state, occurred at higher temperatures with increasing pressure. The cooling rate affected the crystallization process, with higher cooling rates leading to crystallization at lower temperatures. The size of the spherulites decreased with increasing cooling rates. The crystallinity evolution curves showed a linear relationship between the crystallization temperature and pressure. The study used a Kolmogoroff–Avrami–Evans model to describe the evolution into isotropic structures, and the predictions of the model accurately described the effect of pressure and cooling rates on the final spherulite radii.

Keywords: crystallization kinetics; polypropylene; pressure crystallization; pressure dependence of melting points; dilatometry

check for updates

Citation: Speranza, V.; Salomone, R.; Pantani, R. Effects of Pressure and Cooling Rates on Crystallization Behavior and Morphology of Isotactic Polypropylene. *Crystals* **2023**, *13*, 922. https://doi.org/10.3390/cryst13060922

Academic Editor: Jean-Marc Haudin

Received: 4 May 2023
Revised: 1 June 2023
Accepted: 6 June 2023
Published: 8 June 2023

Copyright: © 2023 by the authors. Licensee MDPI, Basel, Switzerland. This article is an open access article distributed under the terms and conditions of the Creative Commons Attribution (CC BY) license (https://creativecommons.org/licenses/by/4.0/).

1. Introduction

Isotactic Polypropylene (iPP) is a widely used polymer due to its excellent mechanical and thermal properties, as well as its chemical resistance. The crystalline structure of polypropylene is one of the most important factors that determines its properties, as the crystal structure affects the mechanical strength, stiffness, and thermal stability of the polymer. The crystallization behavior of polypropylene is influenced by several factors, such as temperature, cooling rate, and pressure [1,2]. Among these factors, pressure has been found to play a crucial role in the evolution of crystallization [3,4]. Understanding the effect of pressure on the crystallization kinetics of iPP is significant for both scientific and technological points of view, since in many industrial processing techniques, e.g., injection molding and compression molding, the polymer solidifies under pressures which can be as high as 1000 bar. Most of the literature papers aimed at assessing the effect of pressure on the crystallization kinetics of iPP use an off-line approach [5–7]: the samples are solidified using a specific thermomechanical protocol involving a given pressure and thermal history, and then analyzed adopting several techniques including microscopy, X-ray diffraction, thermal analysis, and mechanical testing, among others. It is clear that these methods cannot provide data concerning the time evolution of the processes. On the other side, on-line approaches are less frequently reported. These approaches consist in monitoring a property directly related to crystallinity, e.g., heat in

high pressure calorimetry [8] or specific volume in dilatometry [3,9] during the solidification under pressure. This latter approach provides much deeper insight into the evolution of the phenomenon of crystallization, but is generally limited to cooling rates of a few °C/min [10] which are very low if compared with those obtained in commonly adopted processes which are at least of the order of 1 °C/s.

A dilatometer allowing cooling rates of several °C/s was relatively recently introduced [11]. This dilatometer, named Pirouette, allows to monitor in-line the pressure-volume-temperature (PvT) relationship of polymeric samples and to analyze off-line the resulting samples which are not destroyed during the test.

In this work, the effect of cooling rates and pressures on the crystallization kinetics of an iPP is investigated by adopting dilatometric tests conducted in conditions close to the ones experienced by the polymer during the processing. A model for quiescent crystallization that considers the effect of pressure by introducing a melting temperature linearly dependent upon pressure is proposed. Model predictions are compared with crystallinity evolutions during PvT tests and the final morphologies of the pressurized samples.

2. Materials and Methods

A well-characterized iPP, (T30G, Basell, Switzerland) was adopted for all the experimental investigations conducted in this work.

2.1. PvT

Specific volume measurements were performed using a custom made piston-die dilatometer [12]. The apparatus allows isothermal and non-isothermal tests and also shear steps can be applied at predefined thermal history. Ring-shaped samples obtained by a mini-injection molding machine, BABYPLAST 6/10 were used in the piston-die dilatometer. Ring-shaped sample dimensions are 21 mm inner diameter, 22 mm outer diameter and 2.5 mm height. The sample weight is about 60 mg.

Specific volume measurements were conducted in the isobaric cooling mode, according to the protocol outlined in Figure 1. The pressure cell was first heated to 220 °C, adopting a heating rate of about 10 °C/min. After that, it was kept at 220 °C for 10 min to delete all the effect on the sample of the previously applied thermo-mechanical history. Next, the sample was pressurized to the desired value and finally, it was cooled down to a temperature of 40 °C. Pressure was kept constant during the sample cooling. Four different pressure levels were adopted for the specific volume measurements: 100, 200, 400, and 600 bar.

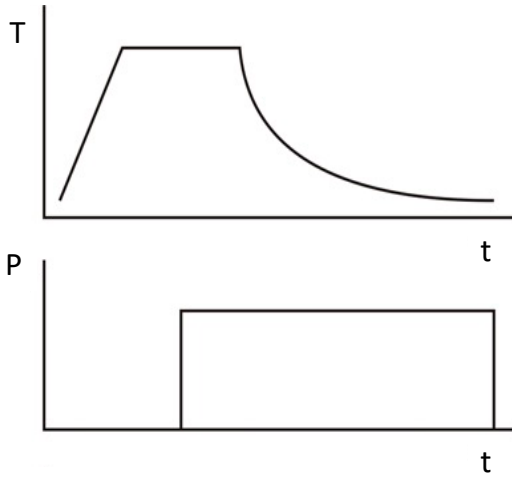


Figure 1. Thermal and pressure protocol adopted during the specific volume measurements.

In order to study the effect of the cooling rate on the specific volume behaviour of the polymer, for each defined pressure level, two different cooling conditions were adopted. In particular, the dilatometer was cooled down to the final temperature passively in free

convection conditions and using as cooling medium compressed air. In both cases, cooling rate decreased during the test, reaching a maximum at the beginning of the test.

2.2. Morphology

The morphology of samples solidified inside the dilatometer was characterized by adopting optical microscopy and X-ray diffraction. By adopting a Leica RM 2165 Microtome equipped with a Cryo-unit Leica LN21, thin slices of 5 µm thickness were obtained at a temperature of −30 °C from the sample according to the cutting scheme depicted in Figure 2.

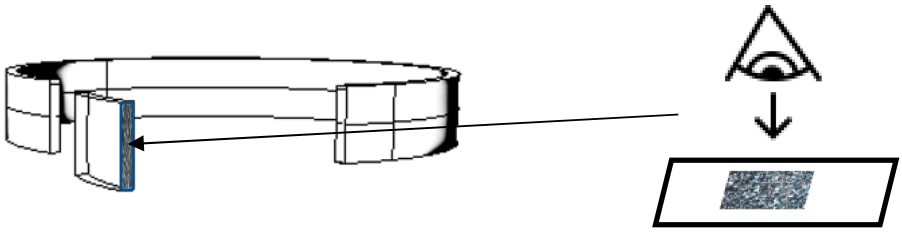


Figure 2. Sketch showing the position of slices adopted for morphology characterization.

Optical micrographs were captured from the slices adopting an Olympus BX 51 microscope equipped with a digital camera. Polarized optical micrographs were analyzed to determine the distribution of spherulites in polymer sample. The optical micrographs were analyzed by freeware software for image analysis, Fiji. Firstly, images were processed to have a better identification of the spherulites in the micrographs. Secondly, the areas occupied by the spherulites were identified, and the equivalent radii were evaluated. Finally, for each condition, the average and the standard deviation of the radii distribution were determined.

Wide angle X-ray scattering (WAXS) patterns from the slices were captured with Bruker D8 ADVANCE. WAXS patterns were analyzed to determine final phase content of some dilatometer samples.

2.3. Differential Scanning Calorimetry

Differential scanning calorimetry was adopted to characterize the specimens obtained by PvT experiments in different processing condition. A differential scanning calorimeter DSC 822 from Mettler-Toledo (Columbus, OH, USA) was adopted to investigate the non-isothermal crystallization. The materials, in the form of pellets, weighing about 4 mg were tested in a nitrogen atmosphere to prevent the degradation of the polymer. The thermal protocol adopted in the non-isothermal tests included a heating stage up to 230 °C conducted with a heating rate of 10 °C/min and a subsequent cooling stage down to the ambient temperature conducted with a cooling rate of −10 °C/min.

3. Results

Dilatometer experiments were carried out with pressure ranging between 100 to 600 bar and two different cooling conditions. In the first condition, the dilatometer was passively cooled in air, whereas in the second, pressurized air was adopted as a cooling medium to cool the dilatometer actively. Figure 3 shows temperature evolutions for two isobaric experiments conducted at 100 bar and adopting the two cooling conditions. As shown in Figure 3, the temperature decreases from 230 to 40 °C during each test following a non-linear behaviour. Cooling rate is maximum at the cooling early stage and then decreases as the time proceeds, assuming a lower value close to the ambient temperature. For the two adopted cooling conditions, cooling was evaluated from the registered thermal histories in the range of crystallization temperature and found to be 0.1 and 1 °C/s, respectively, when the dilatometer is passively and actively cooled.

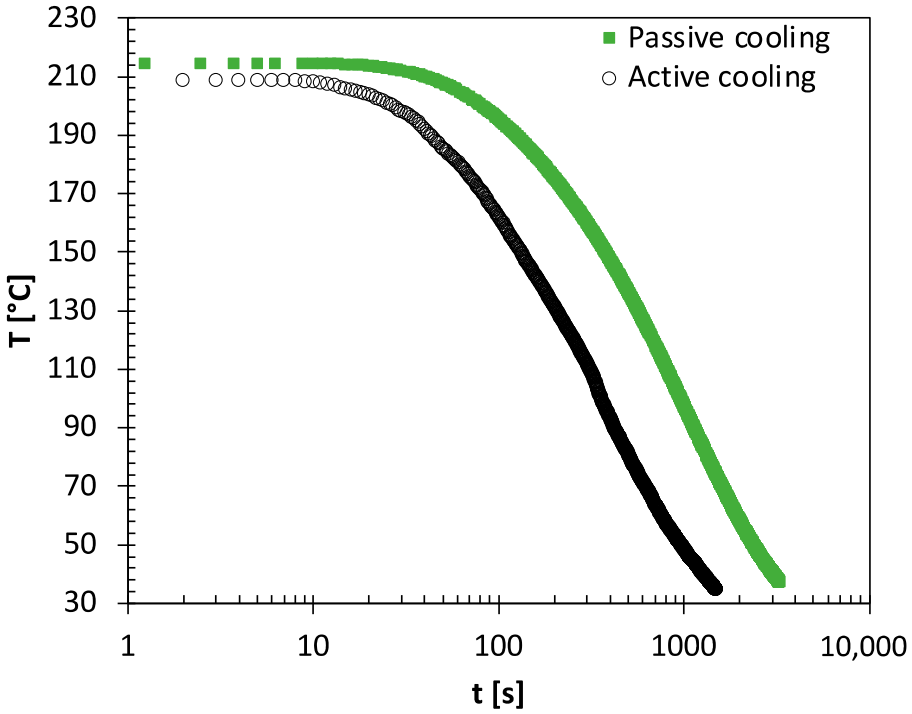


Figure 3. Thermal histories recorded during isobaric cooling test adopting two different cooling conditions.

Figure 4 shows specific volume measurements of iPP at constant pressures of 100, 200, 400, and 600 bar and with an average cooling rate during the crystallization of 0.1 °C/s. Specific volume measurement performed at Gnomix PvT apparatus at 100 bar and with a constant cooling rate of 0.02 °C/s are also reported in Figure 4.

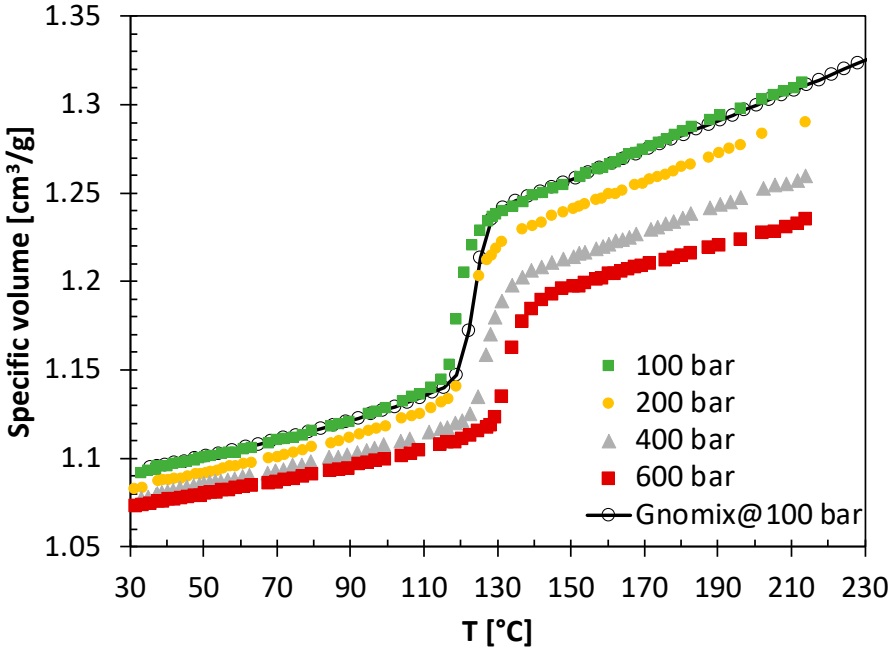


Figure 4. Specific volume of iPP (T30g, Montell) measurements at 100, 200, 400, and 600 bar with piston-die dilatometer with 0.1 °C/s. Measurement with Gnomix dilatometer at 100 bar with a constant cooling rate of 0.02 °C/s are reported for comparison.

Figure 4 shows that changes in specific volumes due to the increase in pressure were larger at high temperatures (namely in melt state) with respect to the increase at low

temperatures (namely in the solid state). Moreover, the polymer crystallization that characterizes the transition between the melt and solid state occurred at higher temperatures by increasing the pressure. The PvT measurements at 100 bar performed with the dilatometer adopted in this work consistently reproduce the results obtained with Gnomix dilatometer. In particular, the molten state results obtained with the two apparatus almost perfectly overlap. The crystallization occurs at higher temperatures in the Gnomix apparatus experiment with respect to this work dilatometer experiment. This can be ascribed to the lower cooling rate experienced by the polymer that shifts the crystallization process to a high temperature. In the solid state, when the crystallization process is completed, results of two experiments are in good agreement. Indeed, cooling rates experienced by the polymer during the two different PvT measurements are not so high to induce different levels of crystallinity in the sample.

Figure 5 shows specific volume measurements of iPP at constant pressures of 100, 200, 400, and 600 bar and with an average cooling rate during the crystallization of 1 °C/s.

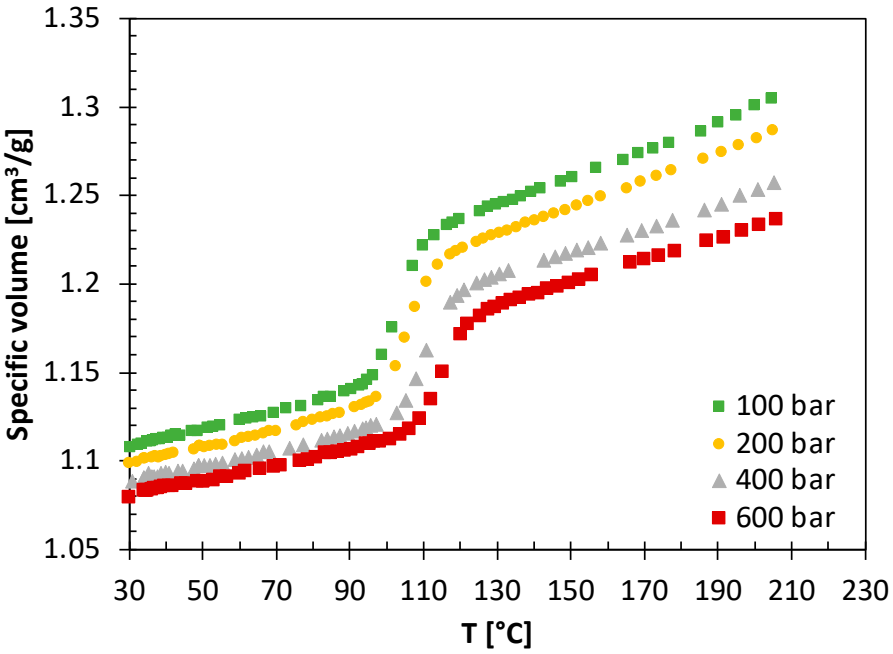


Figure 5. Specific volume of iPP (T30g, Montell) measured in isobaric mode at 100, 200, 400, and 600 bar with piston-die dilatometer with 1 °C/s.

On increasing the cooling rate, for all samples, the crystallization process shifts towards lower temperatures and the transition between polymer melt and solid behaviour spreads over a wider temperature range. This was also confirmed in Figure 6 that shows specific volume of iPP measurements at 600 bar in the two cooling conditions, namely, with estimated cooling rate during the crystallization of 0.1 and 1 °C/s. This phenomenon is due to the fact that the cooling time gets in competition with crystallization kinetics, and thus polymer crystallizes at lower temperatures. Polymer crystallinity can decrease as the cooling rate increases, and thus a specific volume increase would be expected at low temperature. However, such a behaviour is not confirmed by the investigation performed in this work on the samples. Indeed, a small difference between the solid specific volume of the two considered cooling rate was observed at 600 bar. It is worth noticing that a similar behaviour was observed for all the pressures adopted in this work.

Figure 7 shows results of calorimetric measurements performed during heating of the specimens obtained in this work at pressures of 100, 200, 400, and 600 bar and cooling rates of 0.1 and 1 °C/s.

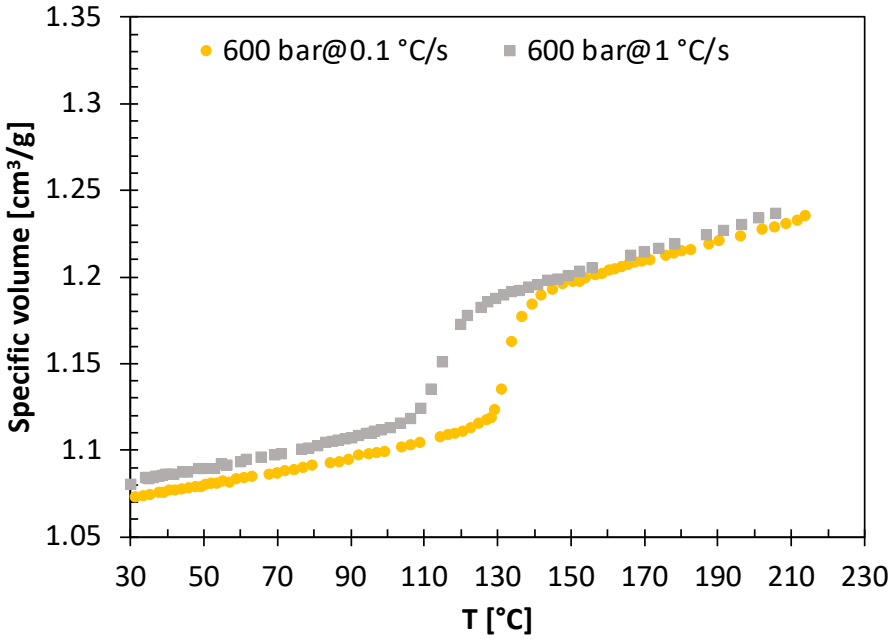


Figure 6. Specific volume of iPP measurements at 600 bar with 0.1 and 1 °C/s.

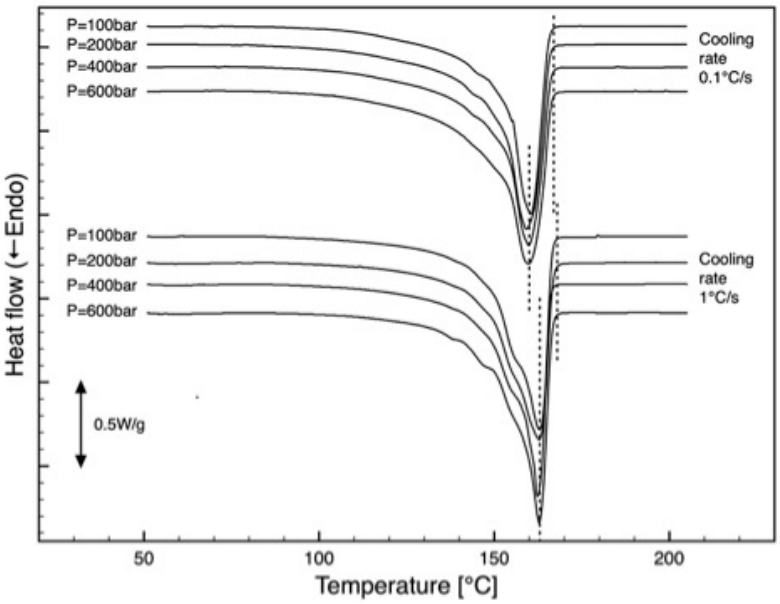
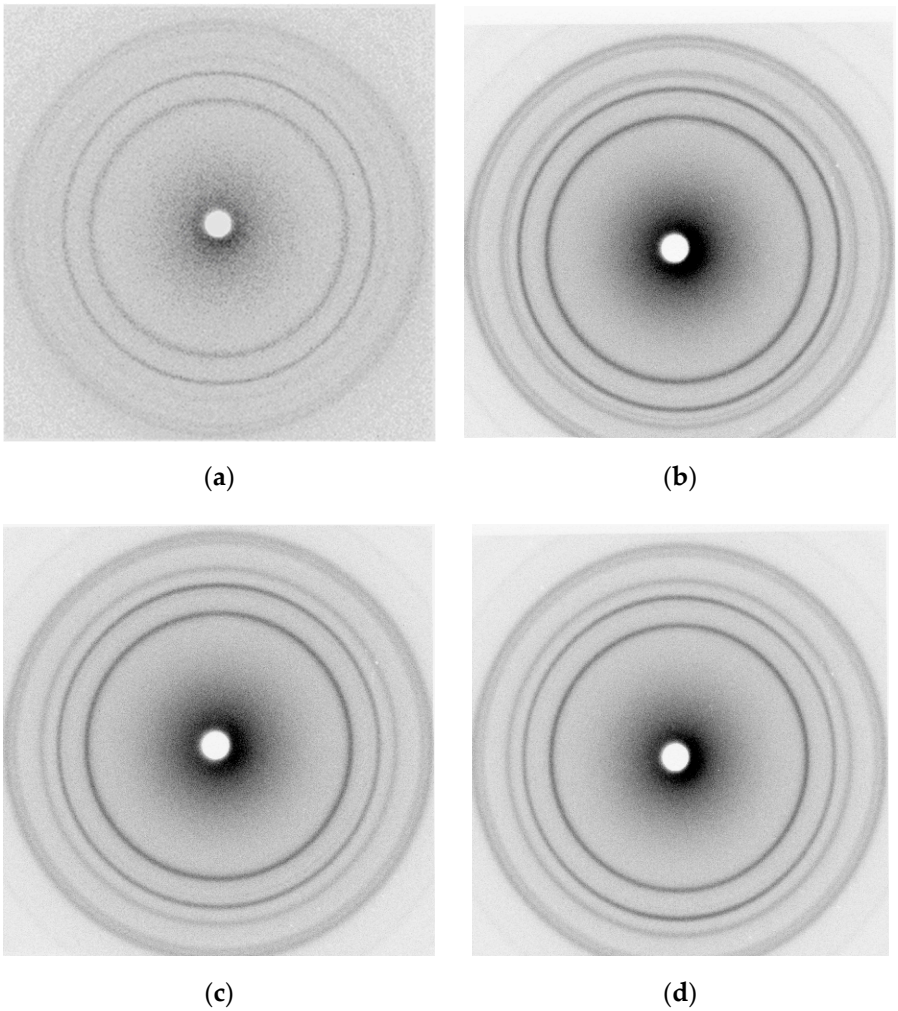


Figure 7. Thermograms collected during heating of the samples solidified under different pressure and temperature histories. In the topmost of the plot are represented thermograms of the samples obtained by cooling the dilatometer passively (namely, characterized by a cooling rate of 0.1 °C/s) whereas in the bottommost of the plot are represented thermograms of the samples obtained by cooling the dilatometer actively (namely, characterized by a cooling rate of 1 °C/s). The vertical dotted lines identify the range of temperatures from the peak to the end of the melting process.

For both considered cooling rates, melting temperature did not change with pressure, but melting occurs at larger temperatures as the pressure increase, which could mean that pressure effect causes the formation of a size distribution of crystals which melt at lower temperatures. Moreover, the peak temperatures were essentially constant with pressure. At higher cooling rates, melting temperatures shift to higher values. Moreover, a double melting peak can be seen. It may be explained as a disorder order transition to partial melting and re-crystallization of crystalline phase.

Figure 8 shows WAXS patterns of samples obtained at 100 and 600 bar pressure and cooling rates of 0.1 and 1 °C/s. For all the considered samples, X-ray diffraction patterns were characterized by concentric rings. This suggests the absence of orientation in the samples and that polymer crystallizes into more isotropic structures, the spherulites.



(**a**) (**b**)

(**c**) (**d**)

Figure 8. WAXS patterns for samples obtained at 100 and 600 bar with cooling rate of 0.1 °C/s (**a**,**b**), and with cooling rate of 1 °C/s (**c**,**d**).

Figure 9 shows polarized optical micrograph of the samples obtained from isobaric tests considered in this work.

As expected, in samples solidified from melt in quiescent conditions, isotropic structures, spherulites, formed. As previously indicated, polymer crystallization shifts to higher temperatures as pressure increases. For the considered iPP, nucleation density decreases as temperature increases. Therefore, a reduction in the size of spherulites would be compatible with a nucleation density that increases by increasing the pressure. Nucleation data at elevated pressures were limited, but first experiments and simulations of Ito et al. ii suggest that nucleation density increases as pressure increases [13,14]. However, in the case of the results of Figure 9, the effect of pressure on the size of the spherulites is not observed. On the other hand, the experiments carried out at 1 °C/s cooling rate showed a reduction in the size of the spherulites. This is consistent with the reduction in crystallization temperatures observed with the high cooling rate. Such a reduction induces an increase in the nucleation density and, thus, a reduction in the spherulite sizes.

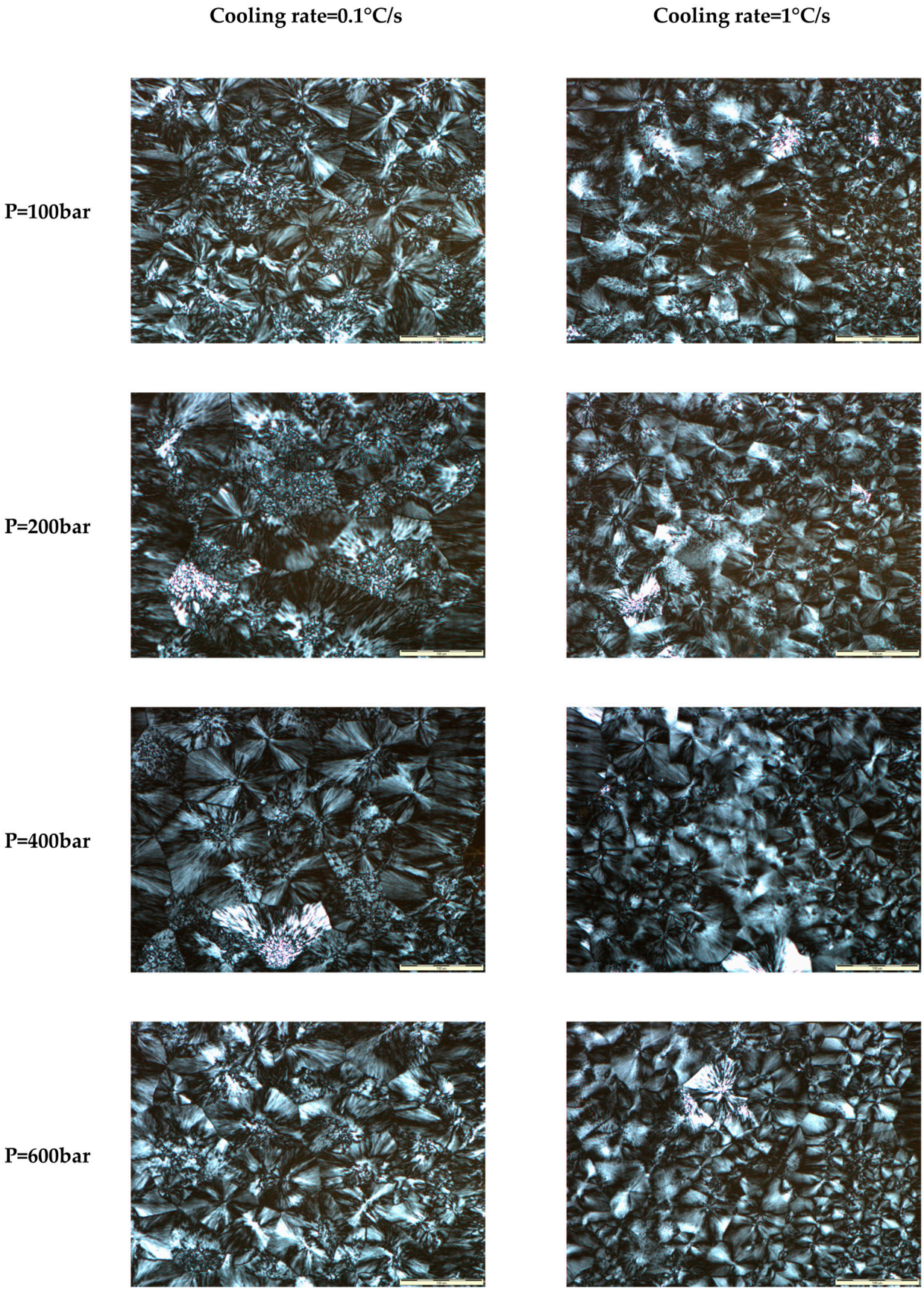


Figure 9. Polarized optical micrograph of the sample obtained from isobaric tests.

4. Discussion

Crystallinity evolutions during the PvT tests can be evaluated from specific volume evolutions with respect to temperature in the transition zone. In particular, for each performed test, the evolution of the relative crystallinity was calculated by the expression

$$relative\ crystallinity = \frac{v(T) - v_m(T)}{v_m(T) - v_s(T)} \quad (1)$$

where $v(T)$ is the specific volume at temperature T as measured with dilatometer, $v_m(T)$ is the specific volume of the melt polymer, and $v_s(T)$ is the specific volume of the solid polymer. Figure 10 shows specific volume evolution for the dilatometer test conducted with 100 bar pressure and cooling rate of 0.1 °C/s.

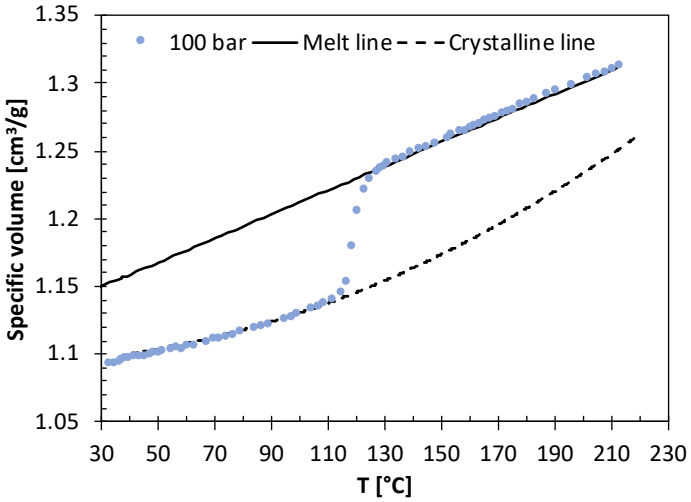


Figure 10. Specific volume of iPP measurement at 100 bar with 0.1 °C/s. Specific volumes of polymer in melt and solid state are represented as solid and dashed lines, respectively.

The specific volume of polymer in melt and solid state over the whole range of temperature adopted in the dilatometer tests can be described with a linear and a polynomial dependence, respectively, and are also shown in the figure with a solid and dashed line.

Figure 11 shows relative crystallinity evolution as evaluated adopting Equation (1) from the dilatometer tests.

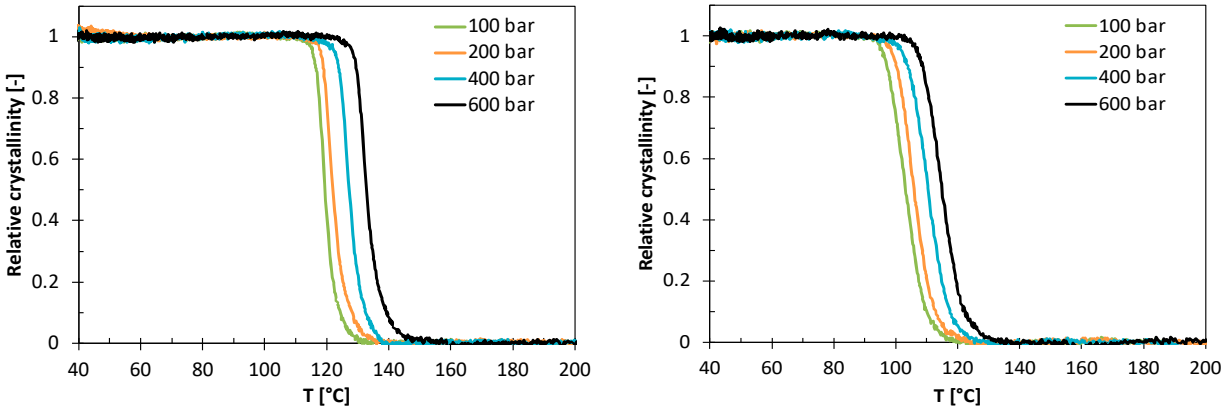
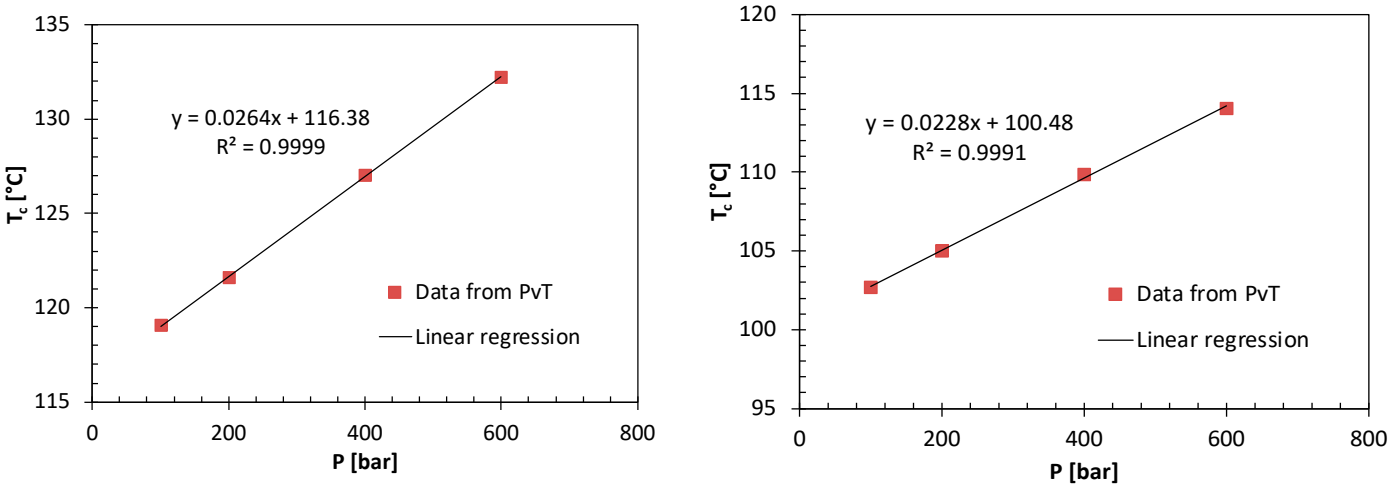


Figure 11. Crystallinity evolution as evaluated from the dilatometer tests adopting Equation (1): (**a**) cooling rate of 0.1 °C/s, (**b**) cooling rate of 1 °C/s.

For each cooling rate, the effect of pressure on the crystallization process is similar: crystallinity started at higher temperatures and moreover it is completed over a broader range of temperatures as the pressure increases. As the cooling rate increases, crystallinity process shifts at lower temperatures and takes place over a wider range of temperatures.

From the crystallinity evolution curves, we evaluated the crystallization temperatures, T_c, at which the 50% of relative crystallinity is attained. Figure 12 shows the dependence of the crystallization temperatures upon pressure for the two adopted cooling rates.

For both the cooling rates, plots evidenced a linear dependence of T_c upon the pressure. In particular, T_c increases with pressure increase. The linear interpolation nicely describes the T_c values for different pressures. The slopes are both positive and very similar; a pressure increase of 100 bar induces a T_c increase of about 2 °C. The value of T_c at atmospheric pressure (intercept at P = 0 of the lines reported in Figure 12) reduces by about 16 °C with the increase of the cooling rate from 0.1 to 1 °C/s.



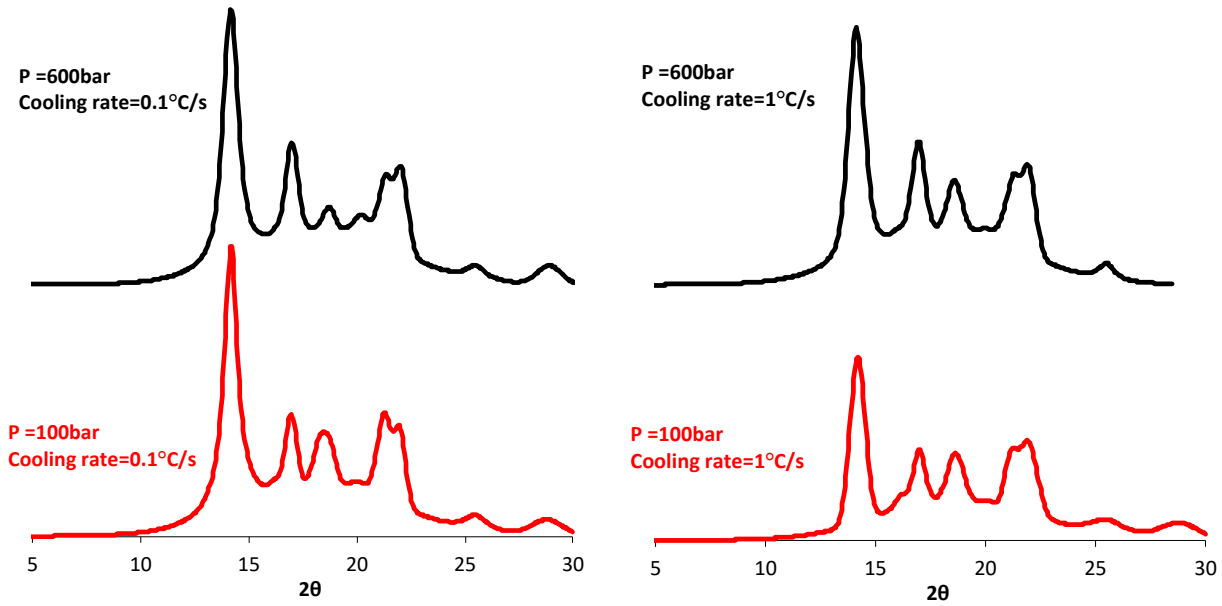
(**a**) (**b**)

Figure 12. Dependence of crystallization temperature upon pressure: (**a**) cooling rate of 0.1 °C/s, (**b**) cooling rate of 1 °C/s.

To evaluate the content of crystalline phases, diffracted intensity patterns were generated by circularly averaging the two-dimensional WAXD patterns shown in Figure 8.

Figure 13 shows the WAXD intensity patterns as a function of the azimuthal angle 2θ of the sample obtained at 100 and 600 bar pressure and with 0.1 and 1 °C/s cooling rates.

In general, iPP presents three different crystalline structures (α monoclinic phase, β hexagonal phase, γ orthorhombic phase), a mesomorphic and an amorphous phase. Every single phase is characterized by several diffractions peaks that appear in well-defined position on WAXS pattern [15]. The plot of the diffracted intensity was analyzed by a deconvolution procedure, as described elsewhere [16,17]. The full spectrum was considered as a superposition of reflections due to the presence of different crystalline fractions. A total number of 12 reflections were considered: 7 for the α phase, corresponding to 2θ = 14.1, 16.9, 18.6, 21.2, 22.1, 25.5, and 28.8; 2 for the mesomorphic form, corresponding to 2θ = 14.5 and 21; 1 for β phase corresponding 2θ = 16 and 1 for the γ form corresponding 2θ = 20.1; 1 for the amorphous halo; each reflection being described by a combination of Lorentzian function and Gaussian function. The overall crystallinity, X_c, was evaluated as the sum of the contribution of the crystalline fractions (α, β, γ, and mesomorphic phase). The error of the measurement was estimated as ±3% on the percentage of each phase. Figure 14 shows the crystalline (mesomorphic phase, α-phase, β-phase, and γ-phase) and amorphous phase content for the samples analyzed with WAXD technique.



(**a**) (**b**)

Figure 13. X-ray diffractograms of samples obtained at 100 and 600 bar pressure: (**a**) cooling rate of 0.1 °C/s, (**b**) cooling rate of 1 °C/s.

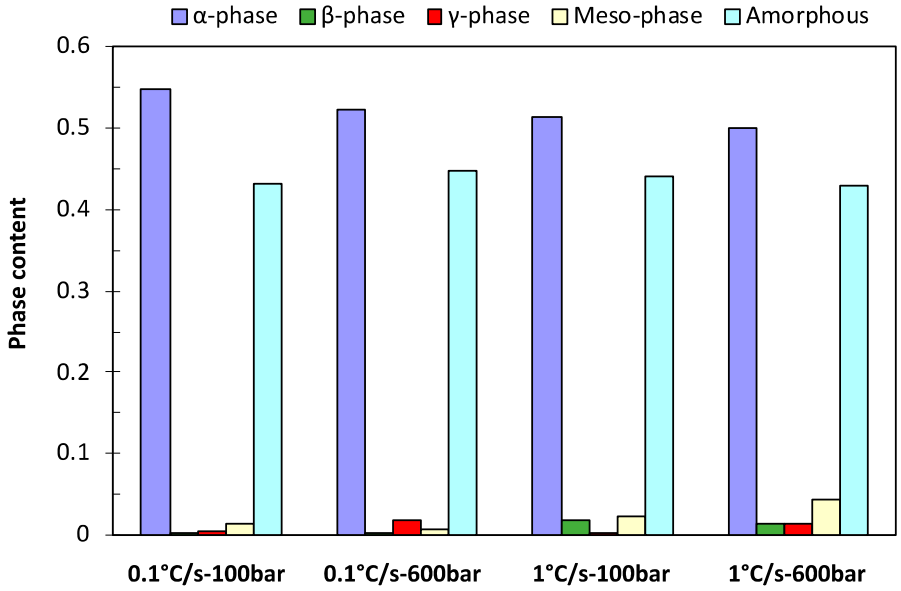


Figure 14. Phase content of samples obtained at 100 and 600 bar pressure with cooling rate of 0.1 °C/s and 1 °C/s.

Total crystallinity content was almost constant at about 55% for all the analyzed samples. As expected for the adopted grade of iPP, the α-phase was the predominant phase, whereas only small fractions of other phases were detected. Although an increase in gamma phase is measured in the sample on increasing pressure, consistently with already observed in the literature [4,18,19], the absolute value is within the experimental error. By increasing the cooling rate, the content of mesomorphic phase increases (assuming values of 2.5% and 4.4% at 100 bar and 600 bar, respectively). The formation of the mesomorphic phase took place as a consequence of a faster cooling that prevents the formation of more

ordered structures and favors the formation of less ordered structures [20,21]. The β-phase fraction was found negligible for all the investigated samples.

A complete model to describe the crystallinity evolution of the α-phase in the considered iPP was recently proposed [22]. A Kolmogoroff–Avrami–Evans (KAE) model was adopted to describe the evolution into isotropic structures. The Avrami model is adopted in order to take into account the impingement and to describe the degree of space filling, ξ

$$\frac{\partial \xi}{\partial t} = (1 - \xi)\frac{\partial \varphi_0}{\partial t} \tag{2}$$

The predicted relative crystallinity, ξ, is defined as the ratio between the absolute crystallinity, χ_c, and its equilibrium value, χ_c^∞, that is equal to 55% for the considered iPP.

The undisturbed volume occupied by spherulites was described by the Kolmogoroff equation

$$\varphi_0(t) = \frac{4}{3}\pi \int_{-\infty}^{t} \frac{dN(s)}{ds}\left[\int_s^t G(u)du\right]^3 ds \tag{3}$$

where N and G are, respectively, the nucleation density and the growth rate of the spherulitic structures. An extensive characterization of the crystallization process of the iPP adopted in this work was already carried out and dependence upon temperature of both crystalline functions were well defined in literature [22,23]. On the contrary, the effect of pressure on the iPP adopted in this work was investigated only on the basis of the analysis of crystalline phase found in the samples after solidification at different pressures and cooling rates [6]. Several authors investigated the effect of pressure on crystallization kinetics of generic iPP. Such an effect was introduced by considering a linear dependence upon pressure of the temperature characteristic of the crystallization process [14,24–26].

The spherulitic nucleation density, under the hypothesis of heterogenous nucleation, is a function of the temperature according to Equation (4)

$$N = \frac{N_0}{(1 + A_n \exp(B_n(T - T_m(P)))} \tag{4}$$

The spherulitic growth rate is described by the Hoffman and Lauritzen equation (Equation (5))

$$G = G_0 \exp\left(-\frac{U}{R(T - T_\infty)}\right)\exp\left(-\frac{K_g(T + T_m(P))}{2T^2(T_m(P) - T)}\right) \tag{5}$$

A shift factor was used for melting temperature to account for the effect of pressure, P, on the crystallization kinetics.

$$T_m(P) = T_{m,0} + a\ P \tag{6}$$

Parameters for crystalline functions and melting temperature expressed by Equations (4)–(6) are reported in Tables 1 and 2, respectively. In Table 2 is also reported the value of the melt temperature at atmospheric pressure, $T_{m,0}$.

Table 1. Parameters describing the temperature dependence of spherulitic nucleation density (Equation (4)).

Parameter	Value
N_0 [nuclei/cm^3]	$1.95 \cdot 10^9$
A_n [–]	$1.3 \cdot 10^8$
B_n [K^{-1}]	0.155

Table 2. Parameters describing the temperature dependence of spherulitic growth rate (Equations (5) and (6)).

Parameter	Value	Value
	Regime I **T < 137 °C**	**Regime II** **T > 137 °C**
U/R [K]	751.6	751.6
G_0 [cm/s]	1380	12.5
K_g [K2]	371,381	257,408.8
$T_{m,0}$ [°C]	194.54	194.54
a [°C/bar]	0.025	0.025
T_∞ [°C]	−74.44	−74.44

As suggested by the analyses of the data collected in this work, melting temperature increase of 2.5 °C for an increase of pressure of 100 bar.

Figure 15 shows a comparison between the experimental relative crystallinity evolutions (shown as solid lines) and model predictions obtained with the KAE model proposed in this work at different pressure and cooling rates (shown as dotted lines).

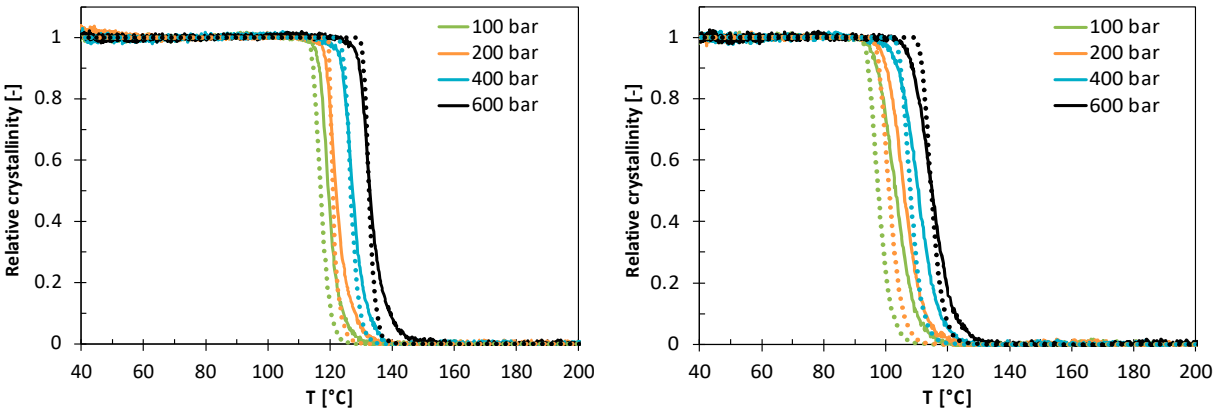
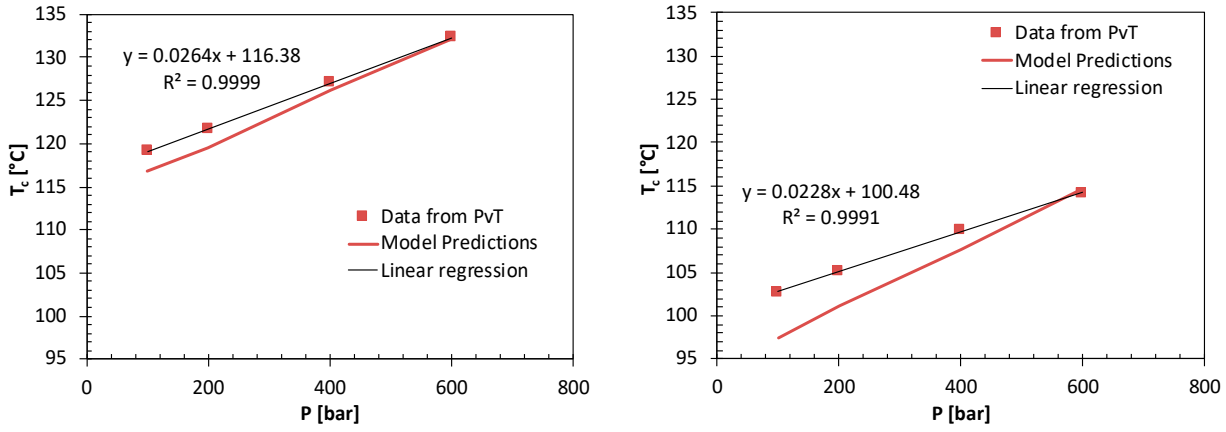


Figure 15. Comparison of experimental relative crystallinity evolutions (solid lines) with model predictions (dotted lines): (**a**) cooling rate of 0.1 °C/s, (**b**) cooling rate of 1 °C/s.

Predictions satisfactorily describe the effect of pressure and cooling rate on the crystallization process. In particular, at a low cooling rate, the enhancement of the crystallization kinetics due to the pressure is consistently captured by the predictions. Description of crystallinity evolutions at a high cooling rate is less accurate. Main features shown by the experimental data are captured by the predictions. The crystallization process occurs at lower temperatures as the cooling rate increases, and higher crystallization temperatures are predicted as pressure increases. It is worth pointing out that this result was obtained by adopting a single parameter linearly dependent upon pressure. Obviously, it would be possible to perfectly interpolate the crystallinity evolution during the PvT tests by considering in the proposed model more parameters dependent upon pressure or introducing more complex dependence of parameters upon pressure. However, this enhancement of the complexity of the model would limit its applicability for the numerical simulation of polymer processing.

Figure 16 shows the comparison of the predicted half crystallization temperatures and the values obtained from the analysis of the isobaric specific volume measurements.

Predictions at the highest pressures are almost correct for both considered cooling rates, whereas half crystallization temperature is underestimated as the pressure decreases, especially at a high cooling rate.



(**a**) (**b**)

Figure 16. Comparison of half crystallization temperatures evaluated from PvT measurements and the predicted values: (**a**) cooling rate of 0.1 °C/s, (**b**) cooling rate of 1 °C/s.

The model proposed to describe the crystallization process of iPP allowed for evaluating the average spherulite radius, R, that can be obtained from Equation (7)

$$R = \sqrt[3]{\frac{3\,\xi}{4\pi\,N_a}} \tag{7}$$

where ξ and N_a refer to the final values. When Kolmogoroff's approach is followed, the number N_a of active nuclei at the end of the crystallization process can be calculated as

$$N_a = \int_0^t \frac{dN_s(p)}{dp}(1-\xi(p))dp \tag{8}$$

Figure 17 shows the comparison of the final spherulites radii evaluated from the analysis of the polarized optical micrographs of the samples and model predictions obtained using Equations (7) and (8).

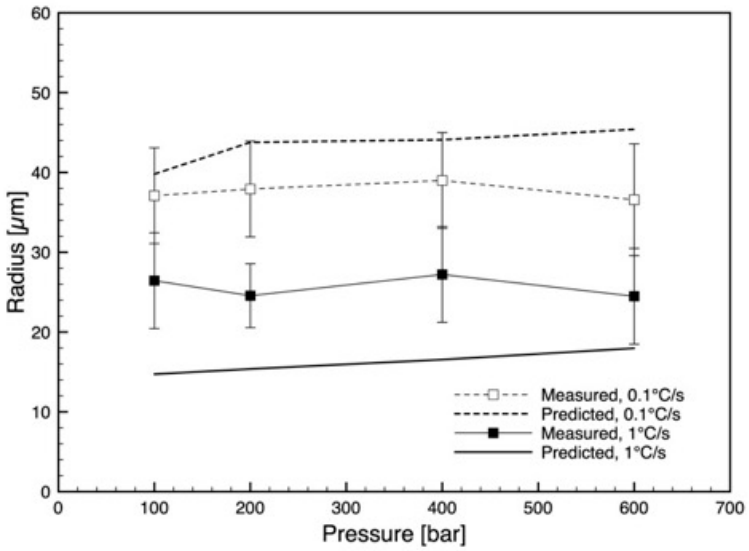


Figure 17. Comparison of the final spherulites radii evaluated from the analysis of the polarized optical micrographs of the samples (shown in Figure 9) and model predictions obtained using Equations (7) and (8).

Predictions were found in good accordance with the experimental data. The effect of pressure and cooling rates on final spherulites radii were correctly described by model predictions. In particular, a cooling rate increase induced a decrease in the predicted final radius.

5. Conclusions

Specific volume measurements were performed using a piston-die dilatometer operated at pressures ranging from 100 to 600 bar and cooling rates of 0.1 and 1 °C/s.

The morphology of the samples solidified inside the dilatometer was characterized by adopting DSC, optical microscopy, and X-ray diffraction.

Changes in specific volumes due to the increase in pressure were larger at high temperatures (namely, in melt state) with respect to the increase at low temperatures (namely, in the solid state). Moreover, the polymer crystallization that characterizes the transition between the melt and solid state occurred at higher temperatures upon increasing the pressure and upon decreasing the cooling rates.

For all the considered samples, X-ray diffraction patterns were characterized by concentric rings. This suggests the absence of orientation in the samples and that polymer crystallizes into isotropic structures. Indeed, the polarized optical micrographs show that only spherulitic structures are formed. It was observed that size of spherulites decreases with the cooling rate increase, whereas no effect of the pressure on the spherulites' size was detected.

For both the cooling rates, a linear dependence of the temperatures, T_c, at which the 50% of relative crystallinity is attained upon the pressure is found: a pressure increase of 100 bar induces a T_c increase of about 2 °C.

The plot of the WAXD patterns was analyzed by a deconvolution procedure. Total crystallinity content was almost constant at about 55% for all the analyzed samples. As expected for the iPP adopted, only small content of crystalline phases β, γ, and meso phases were detected, whereas the predominant phase was the α-phase. An increase in γ-phase, although within the experimental error, was observed in the samples obtained with the highest pressure. This finding was consistent with the fact that the formation of the γ-phase is promoted under high pressure. By increasing the cooling rate, especially with the highest pressure, the content of the mesomorphic phase increases. Indeed, faster cooling prevents the formation of more ordered structures and favors the formation of less ordered structures and thus the formation of the mesomorphic phase.

A Kolmogoroff–Avrami–Evans (KAE) model was adopted to describe the evolution into isotropic structures. The effect of pressure on crystallization kinetics was considered by adopting a melting temperature linearly dependent upon pressure.

Predictions correctly describe the effect of pressure and cooling rate on the crystallization process. In particular, at low cooling rates, the enhancement of the crystallization kinetics due to the pressure is consistently captured by the predictions. Description of crystallinity evolutions at high cooling rates is less accurate.

The effect of cooling rates on final spherulites radii were correctly described by model predictions. In particular, a cooling rate increase induced a decrease in the predicted final radius.

Author Contributions: Conceptualization, V.S. and R.P.; methodology, V.S.; validation, V.S., R.S. and R.P.; investigation, V.S. and R.S.; writing—original draft preparation, V.S.; writing—review and editing, V.S., R.S. and R.P.; supervision, R.P. All authors have read and agreed to the published version of the manuscript.

Funding: This research received no external funding.

Institutional Review Board Statement: Not applicable.

Informed Consent Statement: Not applicable.

Data Availability Statement: The data that support the findings of this study are available from the corresponding author upon reasonable request.

Conflicts of Interest: The authors declare no conflict of interest.

References

1. Wang, J.; Hopmann, C.; Schmitz, M.; Hohlweck, T. Influence of measurement processes on pressure-specific volume-temperature relationships of semi-crystalline polymer: Polypropylene. *Polym. Test.* **2019**, *78*, 105992. [CrossRef]
2. Haudin, J.M.; Boyer, S.A.E. Crystallization of Polymers in Processing Conditions: An Overview. *Int. Polym. Process.* **2017**, *32*, 545–554. [CrossRef]
3. Angelloz, C.; Fulchiron, R.; Douillard, A.; Chabert, B.; Fillit, R.; Vautrin, A.; David, L. Crystallization of Isotactic Polypropylene under High Pressure (γ Phase). *Macromolecules* **2000**, *33*, 4138–4145. [CrossRef]
4. Von Baeckmann, C.; Wilhelm, H.; Spieckermann, F.; Strobel, S.; Polt, G.; Sowinski, P.; Piorkowska, E.; Bismarck, A.; Zehetbauer, M. The influence of crystallization conditions on the macromolecular structure and strength of γ-polypropylene. *Thermochim. Acta* **2019**, *677*, 131–138. [CrossRef]
5. Pantani, R.; Coccorullo, I.; Speranza, V.; Titomanlio, G. Modeling of morphology evolution in the injection molding process of thermoplastic polymers. *Prog. Polym. Sci.* **2005**, *30*, 1185–1222. [CrossRef]
6. Coccorullo, I.; Pantani, R.; Titomanlio, G. Evolution of Morphology of iPP in Processing Conditions. *Int. Polym. Process.* **2005**, *20*, 186–190. [CrossRef]
7. La Carrubba, V.; Brucato, V.; Piccarolo, S. Phenomenological approach to compare the crystallization kinetics of isotactic polypropylene and polyamide-6 under pressure. *J. Polym. Sci. Part B Polym. Phys.* **2002**, *40*, 153–175. [CrossRef]
8. Nakafuku, C. High pressure d.t.a. study on the melting and crystallization of isotactic polypropylene. *Polymer* **1981**, *22*, 1673–1676. [CrossRef]
9. Van Drongelen, M.; Van Erp, T.B.; Peters, G.W.M. Quantification of non-isothermal, multi-phase crystallization of isotactic polypropylene: The influence of cooling rate and pressure. *Polymer* **2012**, *53*, 4758–4769. [CrossRef]
10. Qin, W.; Liu, K.; Xin, Z.; Ling, H.; Zhou, S.; Zhao, S. Zinc pimelate as an effective β-nucleating agent for isotactic polypropylene at elevated pressures and under rapid cooling rates. *Polym. Cryst.* **2020**, *3*, e10132. [CrossRef]
11. Forstner, R.; Peters, G.W.M.; Meijer, H.E.H. A Novel Dilatometer for PVT Measurements of Polymers at High Cooling and Shear Rates. *Int. Polym. Process.* **2009**, *24*, 114–121. [CrossRef]
12. Van der Beek, M.H.E.; Peters, G.W.M.; Meijer, H.E.H. A Dilatometer to Measure the Influence of Cooling Rate and Melt Shearing on Specific Volume. *Int. Polym. Process.* **2005**, *20*, 111–120. [CrossRef]
13. Ito, H.; Tsutsumi, Y.; Minagawa, K.; Takimoto, J.; Koyama, K. Simulations of polymer crystallization under high pressure. *Colloid Polym. Sci.* **1995**, *273*, 811–815. [CrossRef]
14. Ito, H.; Minagawa, K.; Takimoto, J.; Tada, K.; Koyama, K. Effect of Pressure and Shear Stress on Crystallization Behaviors in Injection. *Int. Polym. Process.* **1996**, *11*, 363–368. [CrossRef]
15. Caelers, H.J.M.; Parodi, E.; Cavallo, D.; Peters, G.W.M.; Govaert, L.E. Deformation and failure kinetics of iPP polymorphs. *J. Polym. Sci. Part B Polym. Phys.* **2017**, *55*, 729–747. [CrossRef]
16. Liparoti, S.; Speranza, V.; Titomanlio, G.; Pantani, R. Effect of rapid mold heating on the structure and performance of injection-molded polypropylene. *Polymers* **2020**, *12*, 341. [CrossRef] [PubMed]
17. Murthy, N.S.S.; Minor, H. General procedure for evaluating amorphous scattering and crystallinity from X-ray diffraction scans of semicrystalline polymers. *Polymer* **1990**, *31*, 996–1002. [CrossRef]
18. Kalay, G.; Zhong, Z.; Allan, P.; Bevis, M.J. The occurrence of the γ-phase in injection moulded polypropylene in relation to the processing conditions. *Polymer* **1996**, *37*, 2077–2085. [CrossRef]
19. Sowinski, P.; Piorkowska, E.; Boyer, S.A.E.; Haudin, J.M. High-Pressure Crystallization of iPP Nucleated with 1,3:2,4-bis(3,4-dimethylbenzylidene)sorbitol. *Polymers* **2021**, *13*, 145. [CrossRef]
20. Liparoti, S.; Sorrentino, A.; Guzman, G.; Cakmak, M.; Titomanlio, G. Fast mold surface temperature evolution: Relevance of asymmetric surface heating for morphology of iPP molded samples. *RSC Adv.* **2015**, *5*, 36434–36448. [CrossRef]
21. De Rosa, C.; Auriemma, F.; Galotto, N.G.; Di Girolamo, R. Mesomorphic form of isotactic polypropylene in stereodefective polypropylene: Solid mesophase or liquid-crystal like structure. *Polymer* **2012**, *53*, 2422–2428. [CrossRef]
22. Speranza, V.; Liparoti, S.; Volpe, V.; Titomanlio, G.; Pantani, R. Modelling of morphology development towards spherulites and shish–kebabs: Application to isothermal flow-induced crystallization experiments on isotactic polypropylene. *Polymer* **2020**, *196*, 122459. [CrossRef]
23. Coccorullo, I.; Pantani, R.; Titomanlio, G. Crystallization kinetics and solidified structure in iPP under high cooling rates. *Polymer* **2003**, *44*, 307–318. [CrossRef]
24. Trotignon, J.-P.; Verdu, J. Skin-core structure–fatigue behavior relationships for injection-molded parts of polypropylene. II. Morphology–fatigue behavior relationships. *J. Appl. Polym. Sci.* **1987**, *34*, 19–36. [CrossRef]

25. Trotignon, J.P.; Verdu, J. Skin-core structure–fatigue behavior relationships for injection-molded parts of polypropylene. I. Influence of molecular weight and injection conditions on the morphology. *J. Appl. Polym. Sci.* **1987**, *34*, 1–18. [CrossRef]
26. He, J.; Zoller, P. Poly (ethylene Terephthalate) at Pressures to 200 MPa: Kinetics and Characterization of Products. *J. Polym. Sci. Part B Polym. Phys.* **1994**, *32*, 1049–1067. [CrossRef]

Disclaimer/Publisher's Note: The statements, opinions and data contained in all publications are solely those of the individual author(s) and contributor(s) and not of MDPI and/or the editor(s). MDPI and/or the editor(s) disclaim responsibility for any injury to people or property resulting from any ideas, methods, instructions or products referred to in the content.